Nanoscale

COMMUNICATION

Check for updates

Self-strengthening stimuli-responsive nanocomposite hydrogels†

Elizabeth Howard,‡[a] Minghao Li, [iD] ‡[b] Michael Kozma,[a] Jiayu Zhao[a] and Jinhye Bae [iD] *[a,b,c]

Stimuli-responsive hydrogels with self-strengthening properties are promising for the use of autonomous growth and adaptation systems to the surrounding environments by mimicking biological materials. However, conventional stimuli-responsive hydrogels require structural destruction to initiate mechanochemical reactions to grow new polymeric networks and strengthen themselves. Here we report continuous self-strengthening of a nanocomposite hydrogel composed of poly(*N*-isopropylacrylamide) (PNIPAM) and nanoclay (NC) by using external stimuli such as heat and ionic strength. The internal structures of the NC-PNIPAM hydrogel are rearranged through the swelling–deswelling cycles or immersing in a salt solution, thus its mechanical properties are significantly improved. The effects of concentration of NC in hydrogels, number of swelling–deswelling cycles, and presence of salt in the surrounding environment on the mechanical properties of hydrogels are characterized by nanoindentation and tensile tests. The self-strengthening mechanical performance of the hydrogels is demonstrated by the loading ability. This work may offer promise for applications such as artificial muscles and soft robotics.

[a]*Department of Nanoengineering, University of California, San Diego, La Jolla, CA, 92093, USA. E-mail: j3bae@ucsd.edu*
[b]*Materials Science and Engineering Program, University of California San Diego, La Jolla, CA 92093, USA*
[c]*Chemical Engineering Program, Department of Nanoengineering, University of California, San Diego, La Jolla, CA 92093, USA*
†Electronic supplementary information (ESI) available: Experimental sections and figures. See DOI: https://doi.org/10.1039/d2nr05408f
‡These authors contributed equally.

Jinhye Bae is an Assistant Professor in the Department of NanoEngineering at the University of California San Diego. She received her Ph.D. in Polymer Science and Engineering at the University of Massachusetts Amherst in 2015, then worked in the School of Engineering and Applied Sciences at Harvard University as a Postdoctoral Fellow. Her research focuses on understanding the physical and chemical

Jinhye Bae

properties of polymeric materials to program their shape reconfiguration and responsiveness. Her research interests also include the integration of material characteristics into new structural design and fabrication approaches for applications in biomedical devices, soft robotics, actuators, and sensors.

Nanocomposite hydrogels are networks of hydrated polymer chains containing dispersed nanomaterials.[1] The incorporation of nanomaterials modifies the characteristics of conventional hydrogels by improving the mechanical properties,[2–4] introducing anisotropy,[5–7] and providing new functionalities.[8–10] Specifically, nanocomposite additives have been used to improve the versatility of stimuli-responsive polymers, which can alter their hydrophilicity or solubility in response to environmental temperature,[11,12] pH,[13,14] ionic strength,[15,16] *etc.* Such tunable stimuli-responsive composite polymeric systems can be useful in applications for soft actuators,[17,18] biomimetic materials,[19,20] biomedical devices,[21,22] and sensors.[23,24] Poly(*N*-isopropylacrylamide) (PNIPAM) has been widely studied among stimuli-responsive polymers since PNIPAM-based hydrogels reversibly swell and deswell through temperatures of a lower critical solution temperature (LCST) near human body temperature, usually around 33 °C.[25,26] However, chemically crosslinked PNIPAM hydrogel is generally limited for use in practical applications with its relatively poor mechanical properties, such as its low strength and toughness. Therefore, researchers have incorporated nanoscale additives such as metal nanoparticles,[27,28] graphene oxide,[29,30] and nanoclay (NC) to synthesize nanocomposite hydrogels with enhanced mechanical properties.[31,32] Among various nanocomposite hydrogels, NC-PNIPAM hydrogel pro-

vides a promising aspect due to its unique and homogeneous three-dimensional structures.[33] NC is a synthetic hectorite disk that is 25 nm in diameter and 1 nm in thickness with a negatively charged face and positively charged edge.[34] In aqueous environments, NC can orient in an edge-to-face structure through attractive electrostatic forces, commonly described as a "house-of-cards" structure.[35] Both its ability to form ordered structures in solution and to physically crosslink PNIPAM with hydrogen bonds can improve the mechanical properties of NC-PNIPAM hydrogels, like toughness and extensibility.[36]

Currently, the self-strengthening behavior of nanocomposite hydrogels that their mechanical properties can be improved with use has gained great attraction as living materials. Recent research in producing artificial muscles has shown that hydrogel actuators can be strengthened through training like living muscle tissue.[37,38] These material systems require structural destruction to initiate the chemical reaction, thus forming a new polymer network to achieve self-strengthening. NC-PNIPAM hydrogels can also be strengthened by physical methods such as uniaxial elongation,[39] freezing treatment,[40] and drying treatment.[41] Nevertheless, these methods require applying mechanical force or damaging the original structures. Furthermore, Tong *et al.* reported a mechanical enhancement in NC-PNIPAM hydrogels by a single heat treatment that leads to the formation of a denser microstructure upon deswelling.[42] However, the multiple or cyclic treatments

for continuous self-strengthening of NC-PNIPAM hydrogels to mimic muscle training have not been studied to our best knowledge.

In this work, we demonstrate a non-invasive and non-destructive approach to self-strengthen NC-PNIPAM nanocomposite hydrogels through deswelling–reswelling (DS–RS) cycles, and study its mechanism. The materials and preparation of NC-PNIPAM hydrogel are shown in Fig. 1a. The aqueous NC-PNIPAM precursor solution was prepared by mixing *N*-isopropylacrylamide (NIPAM) as the monomer, methylenebisacrylamide (BIS) as the chemical crosslinker, Irgacure 2959 as the photoinitiator and NC as the physical crosslinker in deionized (DI) water. The NC-PNIPAM precursor was then transferred into a glass mold and exposed to 365 nm ultraviolet (UV) light at an intensity of 180 mW cm^{-2} for 1 min to photopolymerize and photocrosslink NC-PNIPAM hydrogels with a thickness of 1 mm. Further details outlining the NC-PNIPAM preparation process can be found in the ESI.† The NC-PNIPAM hydrogels were prepared with 3, 10, and 17 wt% NC, respectively, denoted as NC-*X* where *X* represents the wt% of NC. Additionally, the NC-PNIPAM hydrogels that were swelled, deswelled, and reswelled in water were abbreviated as NC-*X*-S, NC-*X*-DS, and NC-*X*-RS, respectively, while the NC-PNIPAM hydrogels treated with 0.01 M KCl were abbreviated as NC-*X* KCl. We note that NC-0 was not studied in this work as its crosslinking density was not enough to maintain
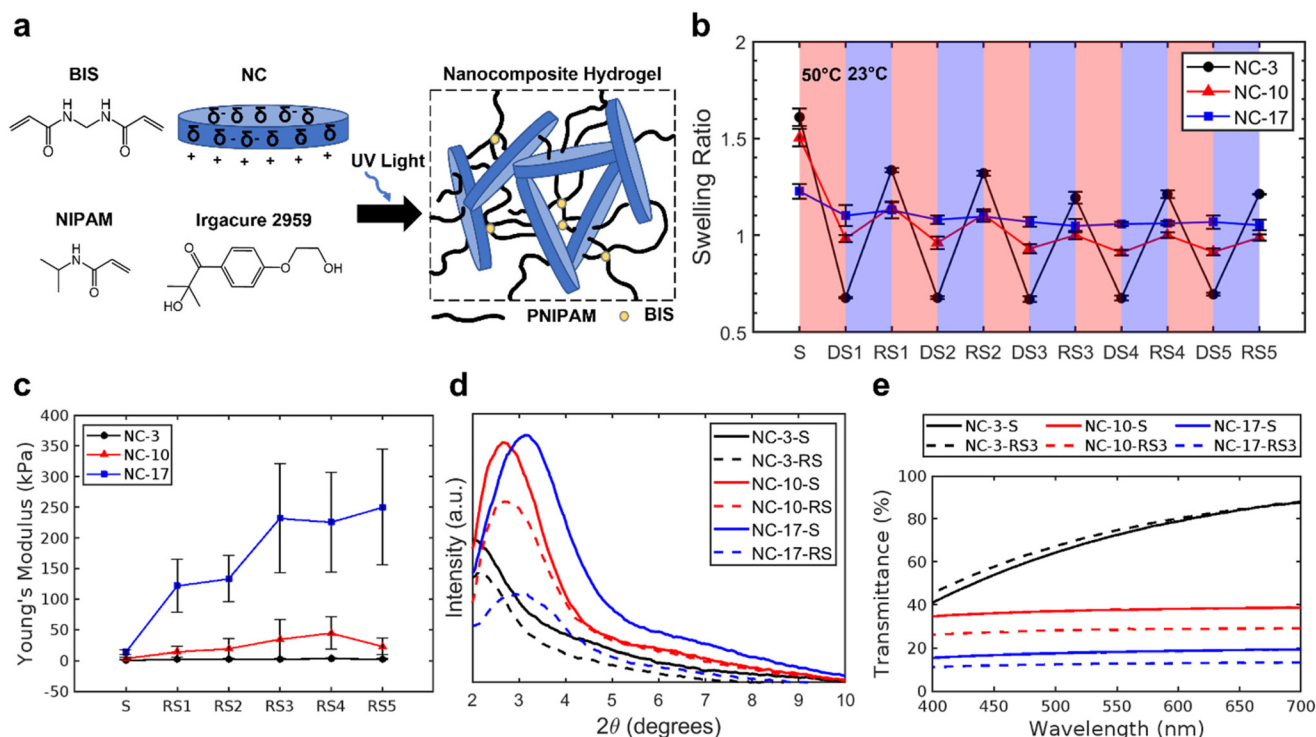

Fig. 1 (a) Schematic illustration of NC-PNIPAM hydrogel fabrication. (b) Swelling ratios of NC-*X* through 5 rounds of DS–RS in 50 °C and 23 °C DI water respectively. (c) Evolution of the Young's modulus of NC-3, NC-10, and NC-17 hydrogels from the swelled state through the fifth reswelled state (RS5). (d) XRD of NC-PNIPAM hydrogels demonstrating a shift in peak position from NC-*X*-S to NC-*X*-RS3. (e) Change in transmittance through NC-*X*-S and NC-*X*-RS3 obtained by UV-Vis spectroscopy.

its form due to no addition of NC as the physical crosslinker (Fig. S1†).

We first characterized the NC-PNIPAM samples at different concentrations of NC through DS–RS cycles after initial swelling. For each NC concentration (NC-3, NC-10 and NC-17), three as-prepared NC-PNIPAM hydrogel disks with a diameter of 5 mm and a thickness of 1 mm were swelled for at least 24 hours in water at 23 °C, then they were moved into a water bath at 50 °C for 24 hours to deswell and a bath at 23 °C for 24 hours to reswell. This timescale allows the NC-PNIPAM hydrogels to reach equilibrium (Fig. S2†), which also agrees with the calculation by the poroelastic diffusion constant for PNIPAM hydrogels ~10^{-11} m^2 s^{-1} regarding a 1 mm hydrogel disk.[26] A hydrogel sample that was initially swelled, then deswelled and reswelled went through one cycle, and was denoted NC-X-RS1, this cycle number increases each time the sample is deswelled and reswelled again. During this process, we measured the swelling ratio as the diameter of the NC-X disk at different cycles divided by the diameter of the as-prepared disk (Fig. 1b). The swelling ratios of the NC-PNIPAM hydrogels were not fully recovered to the initial swelling ratios after DS–RS cycles. Overall, the swelling ratios of the NC-PNIPAM hydrogels decrease until the third cycle (RS3), where they are 26%, 34%, and 15% lower than the initial swelling ratios for the NC-3, NC-10, and NC-17, respectively. This phenomenon manifests that there is an increase in physical crosslinking within the polymer network due to the hydrophobic aggregation of PNIPAM chains which creates more crosslink sites between PNIPAM chains and NC when the temperature is above LCST.[42] We further explored the swelling and deswelling behaviors for NC-PNIPAM with different concentrations of NC by gel weight fractions, $\eta = (W_{23} - W_{dry})/(W_{50} - W_{dry})$, where W_{23} and W_{50} is the weight of hydrogel equilibrated at 23 or 50 °C, respectively, W_{dry} is the weight of the dried hydrogel. The values of η indicate the water absorption ability per unit hydrogel weight between swelling and deswelling states. The result in Table 1 reveals that η has an overall similar trend with the linear swelling ratios in Fig. 1b as η decreases by increasing NC concentration. Next, we measured the Young's moduli of NC-3, NC-10, and NC-17 from the swelled state until the fifth reswelled state (RS5) using nanoindentation to characterize the mechanical properties based on the concentration of NC and the number of DS–RS cycle. Unlike conventional tensile testing, nanoindentation measures the Young's modulus of samples submerged in water at a controlled temperature, so the results were not affected by changes in the swelling ratio due to temperature changes or water evaporation during the measurement. The Young's modulus of NC-PNIPAM increases as NC concentration increases (Fig. 1c), similar to previously reported data, due to the increase in crosslinking density.[43] The Young's modulus continuously increased from the initial swelled state until reaching the third reswelled state (RS3), where NC-3 increased 420% from 0.49 kPa to 2.5 kPa, NC-10 increased 830% from 3.7 kPa to 19 kPa, and NC-17 increased by 1590% from 14 kPa to 230 kPa. Note that the Young's modulus of NC-10 and NC-17 for RS5 are 27.3 ± 11.6 kPa and 258 ± 84.1 kPa, respectively. They are slightly offset to Young's modulus of NC-10 and NC-17 for RS4 as 44.3 ± 26 kPa and 225 ± 81.4 kPa, respectively, but still within the range of the standard deviation of the fourth cycle. We hypothesize that this offset is due to the presence of local aggregation of the NC through DS–RS cycles.

X-ray diffraction (XRD) characterization and transmittance characterization provide insight into the evolving internal interactions of NC-PNIPAM hydrogels during the DS–RS cycles. The XRD peak intensities between the NC-X-S and NC-X-RS3 samples were analyzed using the Bragg equation, $n\lambda = 2d \sin \theta$, where n is the diffraction order, λ is the wavelength, d is the lattice spacing, and θ is the incident angle.[44] Based on the values of 2θ, the d-spacings decrease from NC-3-S = 4.37 nm, NC-10-S = 3.47 nm, and NC-17-S = 2.89 nm to NC-3-RS3 = 4.09 nm, NC-10-RS3 = 3.08 nm, and NC-17-RS3 = 2.72 nm, respectively (Fig. 1d). The result shows the interparticle distance of NC decreases through the DS–RS cycles. This indicates a structural rearrangement is occurring in NC-PNIPAM hydrogels through the DS–RS cycles. Furthermore, through ultraviolet-visible (UV-Vis) spectroscopy examination of NC-X-S and NC-X-RS3, the transmittance decreases from NC-10-S = 37% to NC-10-RS3 = 28% and from NC-17-S = 18% to NC-17-RS3 = 13% while the change in transmittance of NC-3 is not statistically significant (Fig. 1e). In addition, this change in transparency agrees with optical images shown in Fig. S3.† Initially, the transparency of NC-PNIPAM hydrogels after polymerization decreases as the NC concentration increases due to the aggregation of NC.[45] After DS–RS cycles, the further decreasing of the transmittance of NC-PNIPAM hydrogels could be correlated with an increase in inhomogeneity of the crosslinking in the polymer networks through the rearrangement and aggregation of the NC.[46] This result agrees with the XRD data which indicates the decreasing of interparticle spacing between NC through DS–RS cycles.

To further explain the changes in swelling ratio and the Young's modulus of NC-PNIPAM hydrogels through the DS–RS cycles. We correlated the structural rearrangement of the NC-PNIPAM hydrogels with different NC concentrations by the interparticle spacing L and with the diameter of NC (d_{NC} = 30 nm). Here, L is expressed as:[47]

$$L = \frac{V_{NC}\rho_{NC}}{m_{NC}C_{NC}k}$$

where V_{NC}, ρ_{NC}, m_{NC} and C_{NC} are the volume, density, molar mass and concentration of NC, respectively. Here

$$k = \frac{1000}{1000 + (m_{NIPAM}C_{NIPAM}/\rho_{NIPAM}) + (m_{NC}C_{NC}/\rho_{NC})}$$

Table 1 Weight swelling ratios of NC-PNIPAM hydrogels with different NC concentrations

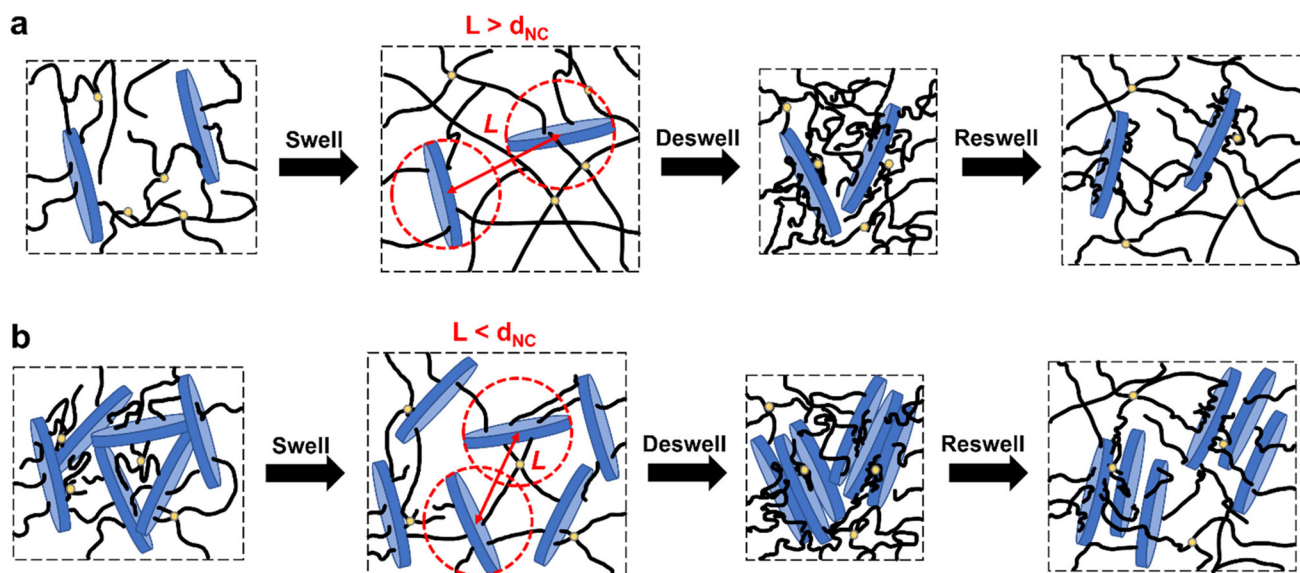| Compsite hydrogel	NC-3	NC-10	NC-17
η	19.4 ± 2.4	2.16 ± 0.10	1.01 ± 0.02

Fig. 2 Schematic illustration of the structural rearrangement for NC–PNIPAM hydrogels through DS–RS cycles: (a) interparticle spacing L is greater than the diameter of NC, more crosslinking points are formed between PNIPAM chains and NC; (b) interparticle spacing L is smaller than the diameter of NC particles, the aggregation (*i.e.*, layer stacking) of NC increases through deswelling process.

where ρ_{NIPAM}, m_{NIPAM} and C_{NIPAM} are the density, molar mass and concentration of NIPAM monomer, respectively; ρ_{NC}, m_{NC}, ρ_{NIPAM} and m_{NIPAM} are 2.65 g cm^{-3} and 762 g mol^{-1},[47] 1.1 g cm^{-3} and 113 g mol^{-1},[48] respectively. The critical concentration of NC for $L = d_{NC}$ is 6.7 wt%. When $L > d_{NC}$, the NC particles could be exfoliated and well distributed in NC-3 hydrogel matrix (Fig. 2a), PNIPAM chains are therefore relatively free to undergo coil-to-globule transition through DS–RS cycles. During the deswelling process, the PNIPAM chains and NC come into closer contact and thus, could form additional crosslinking points between the amide groups on PNIPAM chains and Si–O–Si on the surface of NC.[42] Therefore, the overall crosslinking density increases through the DS–RS cycles, then the swelling ratio decreases and the Young's modulus increases.[41] The swelling ratios and Young's moduli of NC-3 hydrogels equilibrate after three DS–RS cycles which might imply that PNIPAM chains are saturated on the surface of NC. In contrast, NC-10 and NC-17 hydrogel matrices (*i.e.*, $L < d_{NC}$) could induce the spontaneous aggregation of NC by layer stacking during the deswelling process due to restriction by the neighbour NC (Fig. 2b).[47] The NC particles continue to stack through the DS–RS cycles, resulting in more effective crosslinking by both forming more crosslinking points and decreasing the inter-crosslink chain length which causes the increment of the Young's modulus.[41] To support this hypothesis, we have characterized the NC-PNIPAM by small-angle X-ray scattering (SAXS) (Fig. S4†). For NC-3-RS1 and NC-3-RS5, no peak is observed which indicate the uniform distribution of NC within PNIPAM hydrogel matrix through the cyclic treatments. The small peaks for NC-10 and NC-17 represent the inhomogeneities within NC-PNIPAM due to the aggregation of NC.[49] We note that the peak intensity of NC-10-RS5 and NC-17-

RS5 are smaller than NC-10-RS1 and NC-17-RS1, respectively. This can be explained by the scattering functions $I(q) \sim (q^2\xi^2)^{-2}$, where q is the magnitude of the scattering vector and ξ is the characteristic length representing inhomogeneities.[50] The decrease in $I(q)$ implies the increase in ξ, which corresponds to a higher degree of inhomogeneities.[51] The SAXS results explain the evolution of the microstructure changes of the NC-PNIPAM hydrogels as NC particles rearrange and aggregate through the DS–RS cycles.

The internal microstructures of NC-PNIPAM hydrogels with different concentrations of NC in either the swelled or reswelled state were investigated utilizing scanning electron microscopy (SEM). The NC-*X*-S and NC-*X*-RS1 samples were freeze-dried for SEM imaging, following the procedure and analysis detailed in the SEM section of the ESI.† The average pore sizes of diameter decrease from NC-3-S = 14.3 ± 4.7 μm to NC-3-RS1 = 3.4 ± 1.1 μm, from NC-10-S = 17.2 ± 7.8 μm to NC-10-RS1 = 12.7 ± 4.2 μm, and from NC-17-S = 4.7 ± 3.6 μm to NC-17-RS1 = 4.5 ± 4.1 μm (Fig. 3). The decreasing pore size is caused by increasing physical crosslinking points between NC and PNIPAM chains.[47] According to the SEM images, the pore size of the NC-3 samples significantly decreased from the swelled state (S) to the reswelled state (RS). NC-10 and NC-17 showed trivial changes in pore size, but increases in inhomogeneity through the DS–RS cycles (Fig. S5†). Therefore, the energy-dispersive X-ray spectroscopy (EDX) analysis was performed to map the element distribution of NC in PNIPAM. Mg and Si were selected to represent NC (chemical formula $H_{12}Li_2Mg_{16}Na_2O_{72}Si_{24}$). The distribution of NC is highly uniform in NC-3-RS2 whereas NC is aggregated in NC17-RS2 (Fig. S6†). Such results support the mechanisms that the self-strengthening is dominated by the increasing crosslinking
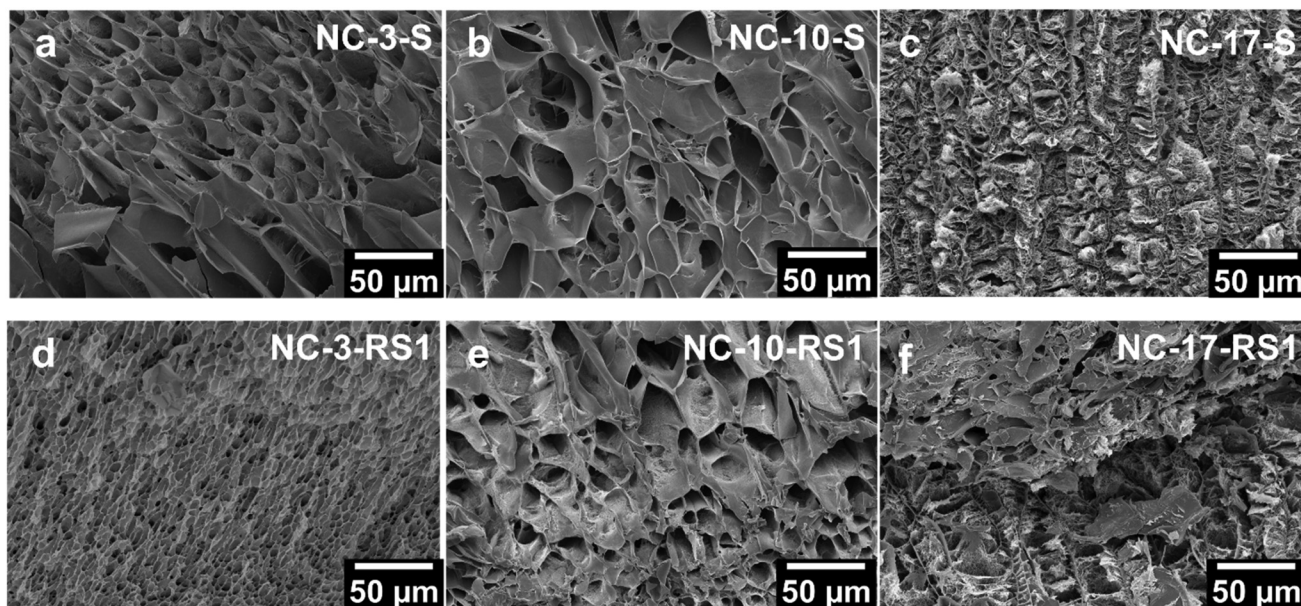
Fig. 3 SEM micrographs of the morphological evolution of NC-PNIPAM from the swelled states of (a) NC-3, (b) NC-10, and (c) NC-17 to the first reswelled states (RS1) of (d) NC-3, (e) NC-10, and (f) NC-17.

points between PNIPAM chains and NC for the low concentration of NC (*i.e.*, NC-3) shown in Fig. 2. However, when the concentration of NC is high (*i.e.*, NC-10 and NC-17), the aggregations of NC lead to the self-strengthening thus their Young's moduli still improve without pronounced pore size change through DS–RS cycles.

Next, we investigated the effect of the ionic strength of the surrounding aqueous environment on the swelling ratio and Young's modulus of NC-PNIPAM to observe the self-strengthening behavior in response to ionic strength. After the NC-*X*-S hydrogels were placed in the 0.01 M KCl for at least 24 hours at 23 °C, their swelling ratio and Young's modulus were measured. Similar to the results of DS–RS cycles, the swelling ratios of NC-PNIPAM hydrogels reduced after KCl treatment by 20%, 36% and 11% for NC-3, NC-10 and NC-17, respectively (Fig. 4a). Furthermore, the Young's modulus increased by

117%, 795% and 278% for NC-3, NC-10 and NC-17, respectively (Fig. 4b), which indicates NC-PNIPAM hydrogels are strengthened by the KCl treatment. We note that the 0.01 M KCl concentration was chosen since it can significantly improve the Young's modulus of NC-PNIPAM hydrogels but not significantly affect the LCST of PNIPAM.[52,53] The self-strengthening mechanism for NC-PNIPAM hydrogels by the KCl treatment is both due to the reduced Debye screening length (λ_D) (Fig. 4c) and the enhanced ionic interaction between NC and PNIPAM chains. Through the permeation of ions, the NC disks are brought closer to each other with a reduced λ_D, which drives water expelling due to osmotic pressure and the NC-PNIPAM hydrogel is thus less swelling.[54] Furthermore, the addition of K$^+$ ions can be absorbed on the negatively charged NC surface and then bonded with the C=O groups on the PNIPAM chains.[52] Therefore, NC-PNIPAM hydro-
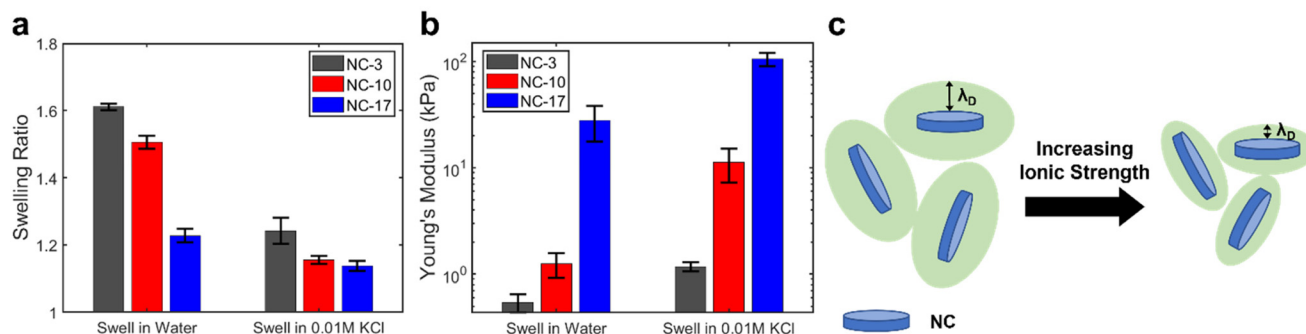

Fig. 4 (a) Comparison of the swelling ratios of NC-*X*-S and NC-*X* KCl. (b) Enhancement of the Young's moduli from NC-*X*-S to NC-*X* KCl, measured through nanoindentation. (c) Schematic of the reduction of the Debye screening length (λ_D) surrounding NC particles as the ionic strength of the medium increases, altering the interparticle interactions.

gels prepared in a salt-free environment undergo a self-strengthening process by increasing the crosslinking density while placed in a salt solution.

We further explored the mechanical properties of NC-*X*-S, NC-*X*-RS1, and NC-*X* KCl through tensile tests and loading tests to understand the self-strengthening effect on the bulk behaviors of NC-PNIPAM. Note that NC-3 was excluded from these bulk experiments since it was not strong enough to undergo tensile and loading tests without deforming or breaking during setup. The toughness and Young's modulus of NC-10 and NC-17 can be deduced from the bulk tensile tests (Fig. 5a). The toughness of NC-10 increased from NC-10-S = 0.063 mJ m^{-3} to NC-10 KCl = 0.13 mJ m^{-3} or NC-10-RS3 = 0.18 mJ m^{-3}. The toughness of NC-17 increased from NC-17-S = 0.13 mJ m^{-3} to NC-17 KCl = 0.24 mJ m^{-3} or NC-17-RS3 = 0.19 mJ m^{-3}. The increases in toughness of NC-PNIPAM hydrogels through DS–RS cycles and KCl treatment, respectively, indicate that the self-strengthening effect increases the amount of energy NC-PNIPAM can absorb without breaking. The Young's modulus of bulk NC-PNIPAM hydrogels increased by 42% from NC-10-S to NC-10 KCl, 105% from NC-10-S to NC-10-RS3, 95% from NC-17-S to NC-17 KCl and 184% from NC-17-S to NC-17-RS3. The increase in toughness and Young's modulus measured by the bulk tensile test indicates that

NC-PNIPAM self-strengthens in response to both DS–RS cycles and exposure to 0.01 M KCl. The average ultimate tensile strength (UTS) was determined by the highest tensile strength achieved by NC-PNIPAM samples before failure. The UTS of NC-PNIPAM hydrogel increases after both the DS–RS cycle and KCl treatment, respectively (Fig. 5b). The average elongation at break was determined by the largest tensile strain achieved before sample failure. This value either remains nearly the same after the third DS–RS cycle and increases when the NC-*X*-S sample is treated with the 0.01 M KCl salt solution (Fig. 5c). The increase in the mechanical properties can be attributed to the increase in overall crosslinking density within NC-PNIPAM hydrogels after undergoing DS–RS cycles or KCl treatments. We attribute the higher elongation at break values of NC-*X* KCl hydrogels to the trapping of nonporous surface structures in water as PNIPAM chains collapse above their LCST, producing voids deeper within NC-PNIPAM where free water aggregates, resulting in a more heterogeneous structure.[26] The load-bearing test demonstrates the variation in elongation length holding the same weight. These hydrogels were cut into rectangular thin strips with a width of 1 cm, length of 6.35 cm, and thickness of 1 mm in the as-prepared state. The NC-10 samples could each support a 37 g load and the length of the sample was reduced by 13% after being treated with 0.01 KCl
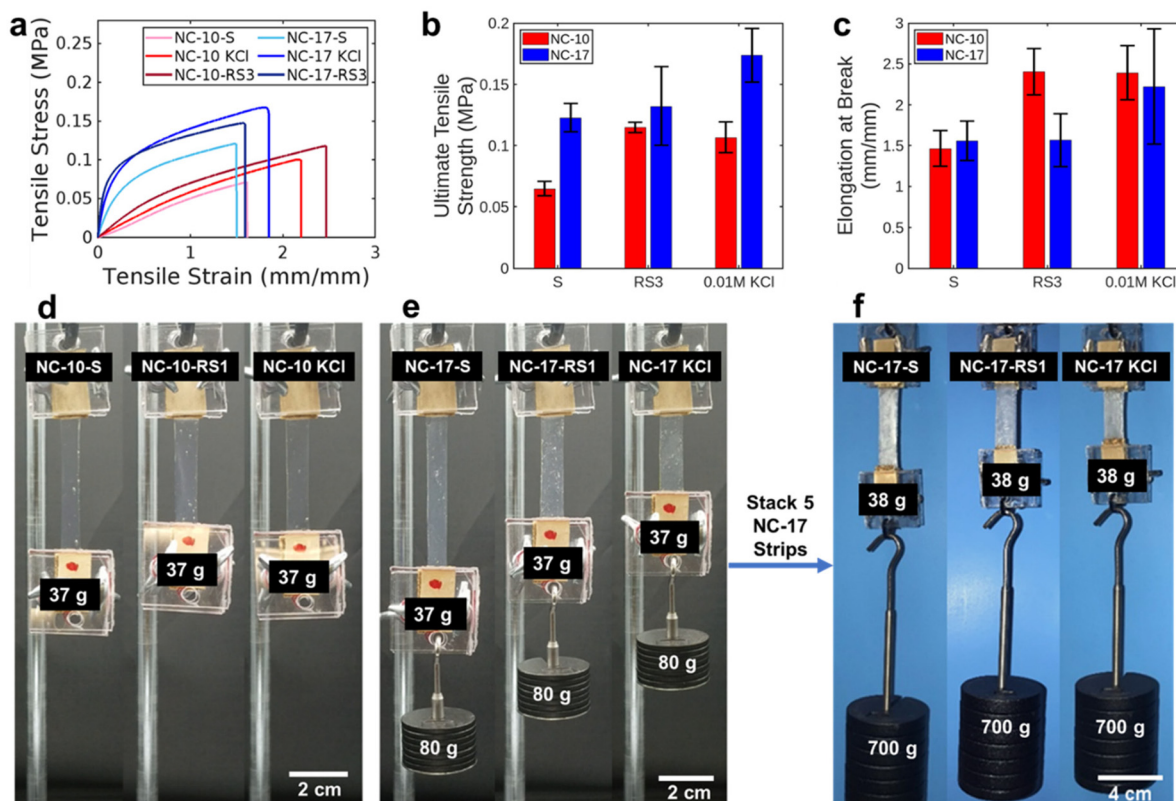

Fig. 5 (a) Stress–strain curves of NC-10-S, NC-10 KCl, NC-10-RS3, NC-17-S, NC-17 KCl, and NC-17-RS3. (b) The average of UTS and (c) the average elongation at break of NC-10-S, NC-10-RS3, NC-10 KCl, NC-17-S, NC-17-RS3, NC-17 KCl. Demonstration of the loading ability of 1 strip of (d) NC-10-S, NC-10-RS1, and NC-10 KCl; and (e) NC-17-S, NC-17-RS1, and NC-17 KCl. (f) Demonstration of the strength enhancement when utilizing 5 strips of NC-17-S, NC-17 KCl, and NC-17-RS1.

and 20% after undergoing DS–RS cycles compared to the swelled state (Fig. 5d). The NC-17 samples can support 117 g and the length of the sample was reduced by 30% after undergoing a DS–RS cycle and 47% after being treated with 0.01 M KCl, compared to the swelled state (Fig. 5e). Furthermore, when 5 strips of NC-17 samples are stacked, they can support a combined total mass of 738 g, which is 6.3 times more than the single NC-17 strip (Fig. 5f). Our samples can fully recover to their original length within a few minutes due to a relatively small deformation (strain <150%). Therefore, utilizing multiple layers of NC-17 enhances the strength, like a muscle, to support a higher combined total mass.

Conclusions

In summary, we reported self-strengthening NC-PNIPAM hydrogels without mechanical stress and structural destruction. Through conformational changes in temperature-sensitive PNIPAM chains during DS–RS cycles, the microstructures change as physical crosslinking increases within NC-PNIPAM hydrogels, and repulsive interactions between NC disks decrease. This self-strengthening effect is reminiscent of the mechanical improvements gained through salt treatments. The increase in the crosslinking density manifests as a lower swelling ratio and higher Young's modulus. This allows us to build new self-strengthening material systems that do not rely on chemical reactions or structural destruction to strengthen, presenting new opportunities for soft robotics, autonomous actuators and artificial tissues.

Conflicts of interest

There are no conflicts to declare.

Acknowledgements

References

1 K. Haraguchi, *Curr. Opin. Solid State Mater. Sci.*, 2007, **11**, 47–54.

2 J. Yang, C.-R. Han, J.-F. Duan, F. Xu and R.-C. Sun, *ACS Appl. Mater. Interfaces*, 2013, **5**, 3199–3207.

3 M. K. Jaiswal, J. R. Xavier, J. K. Carrow, P. Desai, D. Alge and A. K. Gaharwar, *ACS Nano*, 2016, **10**, 246–256.

4 S. Unterman, L. F. Charles, S. E. Strecker, D. Kramarenko, D. Pivovarchik, E. R. Edelman and N. Artzi, *ACS Nano*, 2017, **11**, 2598–2610.

5 K. Hu, J. Sun, Z. Guo, P. Wang, Q. Chen, M. Ma and N. Gu, *Adv. Mater.*, 2015, **27**, 2507–2514.

6 K. Shikinaka, Y. Koizumi and K. Shigehara, *J. Appl. Polym. Sci.*, 2015, **132**, 41691.

7 Q. Luo, Y. Shan, X. Zuo and J. Liu, *RSC Adv.*, 2018, **8**, 13284–13291.

8 X. Zhao, X. Ding, Z. Deng, Z. Zheng, Y. Peng, C. Tian and X. Long, *New J. Chem.*, 2006, **30**, 915–920.

9 R.-C. Luo, Z. H. Lim, W. Li, P. Shi and C.-H. Chen, *ChemComm*, 2014, **50**, 7052–7055.

10 I. Maity, D. B. Rasale and A. K. Das, *Soft Matter*, 2012, **8**, 5301–5308.

11 H. Dai, Q. Chen, H. Qin, Y. Guan, D. Shen, Y. Hua, Y. Tang and J. Xu, *Macromolecules*, 2006, **39**, 6584–6589.

12 Y. Zhou, Y. Cai, X. Hu and Y. Long, *J. Mater. Chem. A*, 2014, **2**, 13550–13555.

13 Y. Zhao, J. Kang and T. Tan, *Polymer*, 2006, **47**, 7702–7710.

14 Z. Han, P. Wang, G. Mao, T. Yin, D. Zhong, B. Yiming, X. Hu, Z. Jia, G. Nian, S. Qu and W. Yang, *ACS Appl. Mater. Interfaces*, 2020, **12**, 12010–12017.

15 R. Zhang, M. Tang, A. Bowyer, R. Eisenthal and J. Hubble, *Biomaterials*, 2005, **26**, 4677–4683.

16 D. Zhang, Y. Fu, L. Huang, Y. Zhang, B. Ren, M. Zhong, J. Yang and J. Zheng, *J. Mater. Chem. B*, 2018, **6**, 950–960.

17 C. Ma, X. Le, X. Tang, J. He, P. Xiao, J. Zheng, H. Xiao, W. Lu, J. Zhang, Y. Huang and T. Chen, *Adv. Funct. Mater.*, 2016, **26**, 8670–8676.

18 J. Zheng, P. Xiao, X. Le, W. Lu, P. Théato, C. Ma, B. Du, J. Zhang, Y. Huang and T. Chen, *J. Mater. Chem. C*, 2018, **6**, 1320–1327.

19 F. Lin, Z. Wang, Y. Shen, L. Tang, P. Zhang, Y. Wang, Y. Chen, B. Huang and B. Lu, *J. Mater. Chem. C*, 2019, **7**, 26442–26455.

20 Q. Yu, J. M. Bauer, J. S. Moore and D. J. Beebe, *Appl. Phys. Lett.*, 2001, **78**, 2589–2591.

21 A. GhavamiNejad, M. SamariKhalaj, L. E. Aguilar, C. H. Park and C. S. Kim, *Sci. Rep.*, 2016, **6**, 33594.

22 R. Kouser, A. Vashist, M. Zafaryab, M. A. Rizvi and S. Ahmad, *ACS Appl. Bio Mater.*, 2018, **1**, 1810–1822.

23 P. Wei, T. Chen, G. Chen, H. Liu, I. T. Mugaanire, K. Hou and M. Zhu, *ACS Appl. Mater. Interfaces*, 2020, **12**, 3068–3079.

24 H. Zhou, Z. Jin, Y. Gao, P. Wu, J. Lai, S. Li, X. Jin, H. Liu, W. Chen, Y. Wu and A. Ma, *Colloids Surf., A*, 2022, **636**, 128113.

25 S. Furyk, Y. Zhang, D. Ortiz-Acosta, P. S. Cremer and D. E. Bergbreiter, *J. Polym. Sci., Part A: Polym. Chem.*, 2006, **44**, 1492–1501.

26 M. Li and J. Bae, *Polym. Chem.*, 2020, **11**, 2332–2338.

27 H. Qin, T. Zhang, H.-N. Li, H.-P. Cong, M. Antonietti and S.-H. Yu, *Chem*, 2017, **3**, 691–705.

28 C. Wang, N. T. Flynn and R. Langer, *Adv. Mater.*, 2004, **16**, 1074–1079.

29 K. Shi, Z. Liu, Y.-Y. Wei, W. Wang, X.-J. Ju, R. Xie and L.-Y. Chu, *ACS Appl. Mater. Interfaces*, 2015, **7**, 27289–27298.

30 X. Ma, Y. Li, W. Wang, Q. Ji and Y. Xia, *Eur. Polym. J.*, 2013, **49**, 389–396.

31 K. Haraguchi, *Colloid Polym. Sci*, 2011, **289**, 455–473.

32 Y. Jin, Y. Shen, J. Yin, J. Qian and Y. Huang, *ACS Appl. Mater. Interfaces*, 2018, **10**, 10461–10470.

33 O. Goncharuk, Y. Samchenko, D. Sternik, L. Kernosenko, T. Poltorats'ka, N. Pasmurtseva, M. Abramov, E. Pakhlov and A. Derylo-Marczewska, *Appl. Nanosci.*, 2020, **10**, 4559–4569.

34 T. Nicolai and S. Cocard, *Langmuir*, 2000, **16**, 8189–8193.

35 Y. Liu, M. Zhu, X. Liu, W. Zhang, B. Sun, Y. Chen and H.-J. P. Adler, *Polymer*, 2006, **47**, 1–5.

36 T. Wang, D. Liu, C. Lian, S. Zheng, X. Liu and Z. Tong, *Soft Matter*, 2012, **8**, 774–783.

37 T. Matsuda, R. Kawakami, R. Namba, T. Nakajima and J. P. Gong, *Science*, 2019, **363**, 504–508.

38 H. Hu, Z. Ma and X. Jia, *Mater. Chem. Front.*, 2020, **4**, 3115–3129.

39 C. Lian, Z. Lin, T. Wang, W. Sun, X. Liu and Z. Tong, *Macromolecules*, 2012, **45**, 7220–7227.

40 S. Zheng, T. Wang, D. Liu, X. Liu, C. Wang and Z. Tong, *Polymer*, 2013, **54**, 1846–1852.

41 K. Haraguchi, H.-j. Li, H.-y. Ren and M. Zhu, *Macromolecules*, 2010, **43**, 9848–9853.

42 C. Lian, Y. Yang, T. Wang, W. Sun, X. Liu and Z. Tong, *Polym. Compos.*, 2016, **37**, 1557–1563.

43 K. Haraguchi, T. Takehisa and S. Fan, *Macromolecules*, 2002, **35**, 10162–10171.

44 P. K. Paul, S. A. Hussain, D. Bhattacharjee and M. Pal, *Bull. Mater. Sci.*, 2013, **36**, 361–366.

45 K. Haraguchi and H.-J. Li, *Macromolecules*, 2006, **39**, 1898–1905.

46 T. Wang, D. Liu, C. Lian, S. Zheng, X. Liu, C. Wang and Z. Tong, *React. Funct. Polym.*, 2011, **71**, 447–454.

47 K. Haraguchi, H.-J. Li, L. Song and K. Murata, *Macromolecules*, 2007, **40**, 6973–6980.

48 H. G. Schild, *Prog. Polym. Sci.*, 1992, **17**, 163–249.

49 Z.-Z. Tong, B. Zhou, J. Huang, J.-T. Xu and Z.-Q. Fan, *RSC Adv.*, 2014, **4**, 15678–15688.

50 M. Shibayama, J. Suda, T. Karino, S. Okabe, T. Takehisa and K. Haraguchi, *Macromolecules*, 2004, **37**, 9606–9612.

51 H. Takeno, Y. Aoki and K. Kimura, *Colloids Surf., A*, 2021, **630**, 127592.

52 P.-I. Au, S. Hassan, J. Liu and Y.-K. Leong, *Chem. Eng. Res. Des.*, 2015, **101**, 65–73.

53 A. Shahin and Y. M. Joshi, *Langmuir*, 2010, **26**, 4219–4225.

54 J. Wang, Z. Chen, X. Li, M. Liu, Y. Zhu and L. Jiang, *ACS Appl. Mater. Interfaces*, 2019, **11**, 41659–41667.